

**1.1 INTRODUCTION**

Carbide-free nanostructured bainite exhibits combination of mechanical properties of strength, hardness, toughness, wear, corrosion and fatigue resistance because of which they are finding applications in the area of rail [1], bearing, armour [2] and power transmission shafts. The combination of mechanical properties is a strong function of composition of the alloy, type and amounts of phases and their size, size distribution and morphology. In a high carbon bainitic steel, strength and hardness improve with increasing amount of bainite but decreases with retained austenite. Though ductility and toughness of nanostructured bainite are enhanced with increased retained austenite, they are complex functions of amount, morphology, stability and composition of retained austenite. Wear resistance increases with increasing strength, hardness, toughness as well as ductility. Fatigue resistance also increases with increasing strength and ductility. Corrosion resistance of nanostructured bainitic steel increases with decreasing amount and size of blocky retained austenite. There is a need to find composition of alloy, combination of phases and its content, its morphology, size and size distribution to get high strength, hardness, ductility, toughness with good wear, fatigue and corrosion resistance in high carbon nanostructured bainitic steels.

This chapter discusses about the brief history of bainite, its types,  $T_0$  curve, mechanisms, microstructure and tensile, fatigue, impact, tribological and corrosion behaviours of nanostructured bainitic steels, knowledge gaps and objectives of the present investigation.

## 1.2 BRIEF HISTORY OF BAINITIC STEEL

Davenport and Bain first identified the bainitic microstructure as a result of systematic isothermal transformation experiments [3]. They reported the discovery of a “acicular, dark etching aggregate” formed after isothermal holding between the temperatures for pearlite and martensite formation. The microstructures were distinct from martensite and pearlite observed in the same steel (Figure 1.1) [4], and they were found to be represented by their own 'C-curve' on the time–temperature–transformation (TTT) diagrams, which they introduced as a convenient way to represent the time dependence of transformation at different temperatures. They hypothesized that the novel microstructure "forms in a manner similar to martensite but becomes increasingly tempered and precipitates carbon”.

Hultgren also proposed, in describing the bainitic structure, that 'needles of troostite' (later renamed bainite) initially formed as martensite needles that were then self-tempered, able to reject carbon and form carbides due to a higher transformation temperature than that associated with martensite [5]. Acicular or plate shapes are frequently the consequence of a displacive transformation. Therefore, an explanation was sought for the slow transformation of bainite relative to martensite. The martensite transformation is typically so rapid that it is frequently considered to be temperature-independent [6]. Robertson studied the transformation rate of the microstructures formed by quenching austenite and postulated that the gradual growth of the ferritic component of bainite is best explained by carbon diffusion regulating transformation [7]. Other research emphasized bainite's resemblance to martensite, and it was understood that bainite formed when carbon was supersaturated [8-11]. Vilella [12] and Bain [13] postulated that transformation involves the abrupt formation of flat plates, followed by

decarburization at a rate proportional to temperature. It was thought that the procedure to remove carbon from the 'quasi-martensite' would take a millionth of a second.

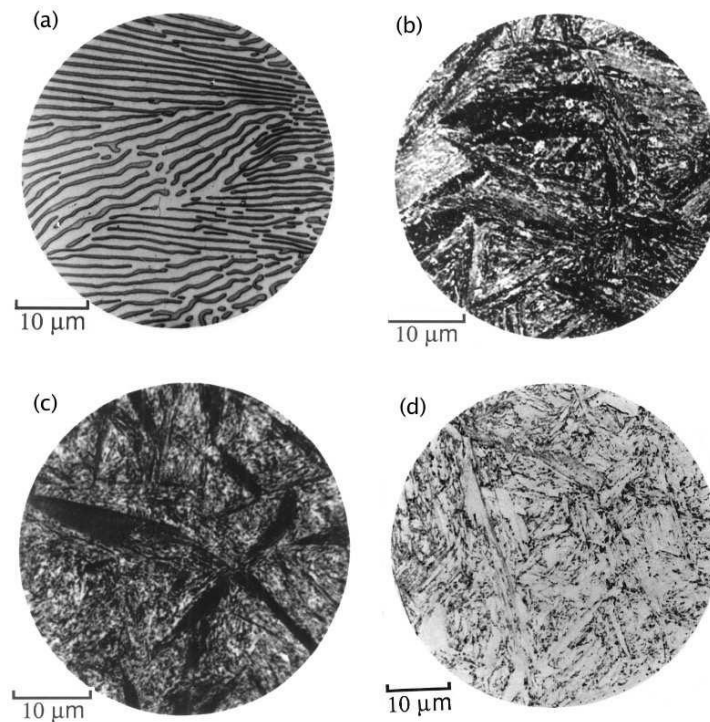


**Figure 1.1** Microstructures in a eutectoid steel. (a) Pearlite formed at 720°C (b) bainite formed at 290°C (c) bainite formed at 180°C (d) martensite [4].

### 1.2.1 Types of Bainite

As depicted in Figure 1.2, it was determined that the form of bainite differed at varying temperature ranges. Mehl introduced the upper and lower bainite classifications, lower bainite transforming at lower temperatures than upper bainite [14]. Upper bainite was previously known as wispy bainite [6]. Figures 1.3a and Figure 1.3b depict upper and lower bainite, respectively. Lower bainite resembles tempered high-carbon martensites under an optical microscope, whereas upper bainite resembles low-carbon martensites [15]. Transmission electron microscopy (Figure 1.4) later demonstrated conclusively that the various varieties are a result of the character of carbide precipitation and can be affected by varying carbon content and temperature. Carbides precipitate from

austenite between plates that have become carbon-enriched in upper bainite, while the upper bainitic ferrite remains carbide-free. Within the ferrite plates of lower bainite is a finer dispersion of plate-like carbides. Carbides have been observed to precipitate in a single crystallographic form within a given ferrite plate, whereas martensite tempering typically results in the precipitation of numerous forms [16].

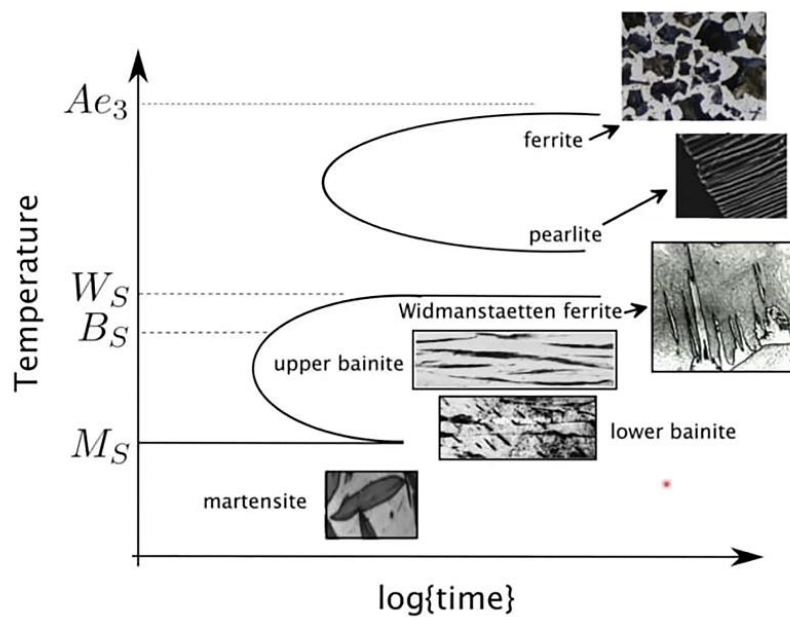
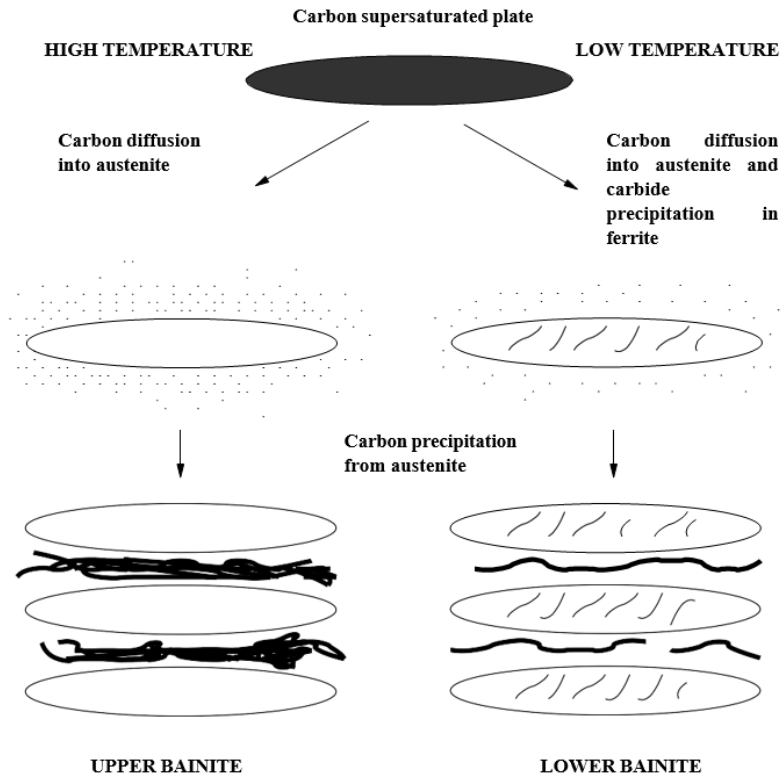


**Figure 1.2** Time temperature transformation (TTT) diagram [17].



+

**Figure 1.3** Growth and development of upper or lower bainite [18].

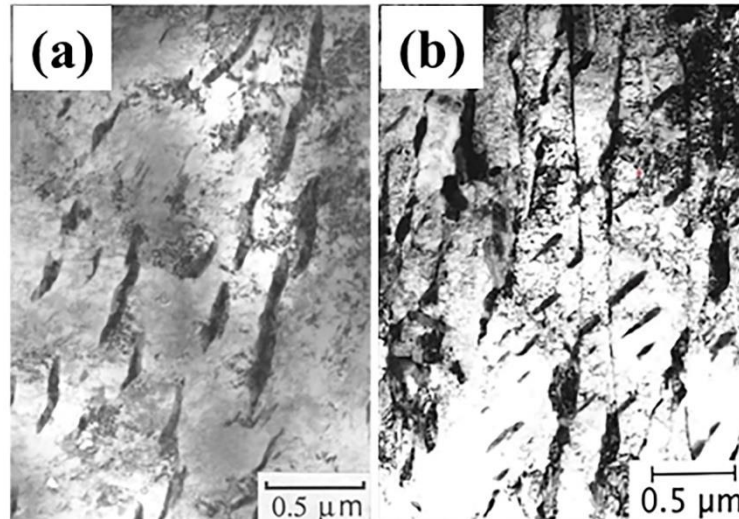


**Figure 1.4** Transmission electron micrographs of bainite (a) upper bainite and (b) lower bainite [19].

In steels where the transformation to pearlite could be delayed, it was observed that the maximal degree of bainite transformation decreased with increasing temperature [20, 21] and that there was a critical temperature above which bainite did not form. Below

this temperature, the transformation to bainite frequently ceases and pearlite forms [21]. Dilatometric experiments on a variety of steels with varying carbon contents revealed that undercooling increased the total expansion. Higher carbon content led to transformation at lower temperatures, resulting in higher expansion during transformation [22]. In each instance, the bainite transformation stopped before the austenite was completely consumed, despite the fact that the steels could continue to transform into pearlite when elevated to a higher temperature.

According to X-ray diffraction, the austenite remaining in steels exhibiting this incomplete reaction phenomenon contained more carbon. This was interpreted by Klier and Lyman to mean that the austenite decomposed prior to the bainite transformation, into carbon-poor and carbon-rich zones [21]. Kurdjumov had made a similar suggestion regarding the transformation of Widmanstätten ferrite [23]. Later, Entin [24] adopted the concept, but Aaronson et al. [25, 26] demonstrated that austenite cannot undergo spontaneous spinodal decomposition. However, this does not rule out random fluctuations in composition, which may play a role in nucleation.

### 1.2.2 $T_0$ Curve

Zener presented a thermodynamic description of the phase transitions in steels [27, 28]. For bainite, he postulated that bainite growth is diffusionless, with any subsequent carbon oversaturation in the ferrite partitioning into residual austenite after growth. In contrast to martensite, bainite would develop without introducing a strain into the microstructure and, consequently, without requiring additional energy as a propelling force. Therefore, bainite would form below the temperature at which austenite and ferrite of the same composition have the same free energy ( $T_0$ ; Figure 1.5). This explained the critical temperature for the formation of bainite, but Zener explained the incomplete

transformation as a result of carbide precipitation, advance of the bainite growth front. Later, Wever and Lange extrapolated the ferrite/ferrite + austenite phase boundary to lower temperatures, which helped to explain the “incomplete reaction” [29]. During isothermal transformation, austenite is enriched with carbon until the locus of  $T_0$  curve is reached, at which point the process cannot continue.

The supersaturation of carbon results in the formation of a plate (or subunit) of bainite, which is then rejected into the residual austenite. The subsequent stratum of bainite must then form from the carbon-rich austenite. This process must end when the concentration of austenite carbon reaches the  $T_0$  curve, as nucleation of the next ferrite plate is thermodynamically unfavourable. If the reaction occurred via diffusion, the ferrite would continue to expand until the carbon concentration reached a para-equilibrium, and the transformation would continue until the carbon concentration of austenite reached the  $Ae_3$  curve.

As observed experimentally, as a result of the  $T_0$  curve, increased volume fractions of bainite can be obtained by transformation at lower temperatures, whereas the equilibrium carbon concentration of austenite given by the  $Ae_3$  curve cannot be attained. After the sample has been cooled to ambient temperature, the remaining austenite can undergo additional transformations or be retained. The austenite can also be present in large volumes where little bainite has formed “blocky austenite” and as thin layers between the bainitic ferrite plates. Important for the mechanical properties of the steel are the final form of the retained austenite, as well as its morphology and composition, which affect susceptibility and the consequences of further transformation to martensite during deformation.

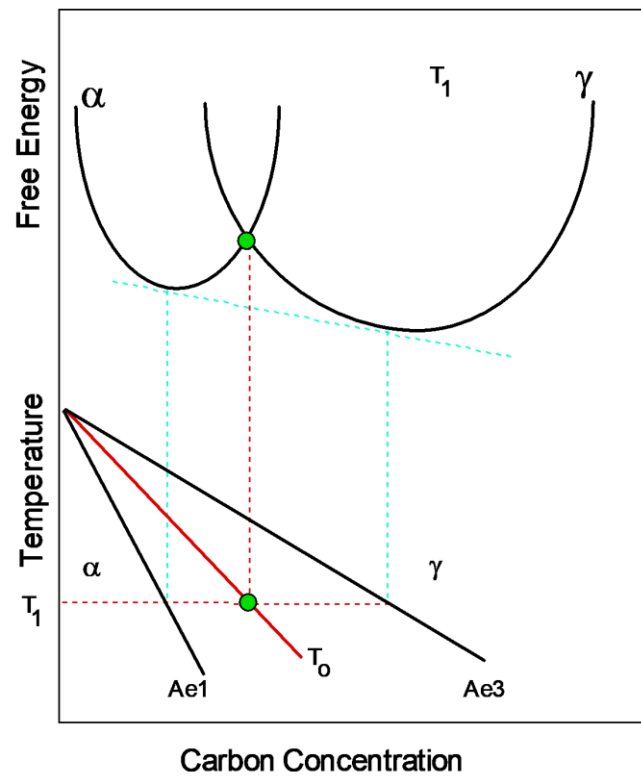


**Figure 1.5**  $T_0$  construction on the Fe-C phase diagram [30].

### 1.2.3 Mechanism of Bainite Formation

Ko and Cottrell [31] investigated the bainite transformation in situ using a heated stage microscope and reported martensite-like surface relief. Plates also ceased growing when they reached the grain boundaries of austenite, which is not required for reconstructive transformations. Surface relief is consistent with a displacive transformation mechanism, while observed sluggish growth rates support the notion that transformation is governed by diffusion.

Oblak and Hehemann [15] rationalized the seemingly contradictory observations by examining the microstructures formed using electron microscopy and noting that the microstructural unit was smaller than previously accepted. The apparent sluggish growth rates at the macroscopic scale can now be attributed to the growth of bainite through the repeated nucleation of sub-units, each of which grows to a finite size very quickly. The

features that were believed to be plates were in fact 'sheaves' or 'packets', aggregate structures composed of these smaller sub-units or platelets [32]. Figure 1.6 is a schematic representation of the observed structures. The macroscopic growth rate of the sheaf is consequently slower than the martensite transformation because it is largely controlled by the nucleation rate of these sub-units, despite the fact that they transform by a martensitic mechanism, forming acicular parallel plates approximately 0.2-0.5  $\mu\text{m}$  in width and 1-10  $\mu\text{m}$  in length.

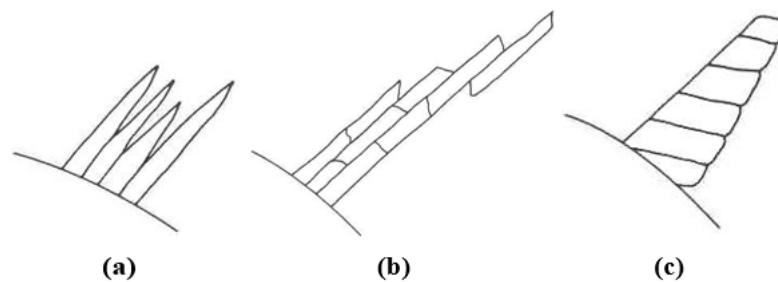


**Figure 1.6** Schematic illustration of structures produced by (a) diffusion-controlled growth, (b) and (c) repeated nucleation of sub-units which rapidly attain a limiting size, after Oblak and Hehemann [15].

The mechanism of bainite formation was also elucidated by Harry Bhadeshia [33]. Bhadeshia's work contributed significantly to understanding the kinetics and mechanisms of bainite formation. The formation of bainite involves the decomposition of austenite, the high-temperature phase of steel, into two distinct phases: ferrite and cementite. This decomposition occurs at temperatures below the pearlite transformation temperature and above the martensite transformation temperature. The primary mechanism proposed by Bhadeshia for bainite formation is the displacive transformation, which involves the cooperative movement of atoms in the crystal lattice. The process can be divided into two stages: nucleation & growth, and carbon diffusion.

1. Nucleation and growth: Bainite nucleate at specific sites within the austenite matrix, which are often associated with crystal defects such as grain boundaries, dislocations, and interfaces with non-metallic inclusions. These sites act as preferential nucleation sites for the new phases. Nucleation takes place by carbon partitioning and growth of ferrite occurs at fast rate by a diffusionless shear process or displacive mechanism to supersaturated ferrite plate. The growth is accompanied by a shape deformation which is an invariant–plane strain with a large shear component
2. Carbon diffusion: Carbon atoms partition into the residual austenite (or precipitate as carbides), shortly after growth is arrested. Internal precipitation of carbides within this supersaturated bainitic ferrite is a subsequent stage of reaction. More sluggish reaction type carbides are precipitated between the bainitic ferrite platelets by decomposition of the carbon rich residual austenite. Carbon diffusion is relatively slow in bainite compared to other microstructures like pearlite, resulting in a fine and needle-like morphology (Figure 1.7).

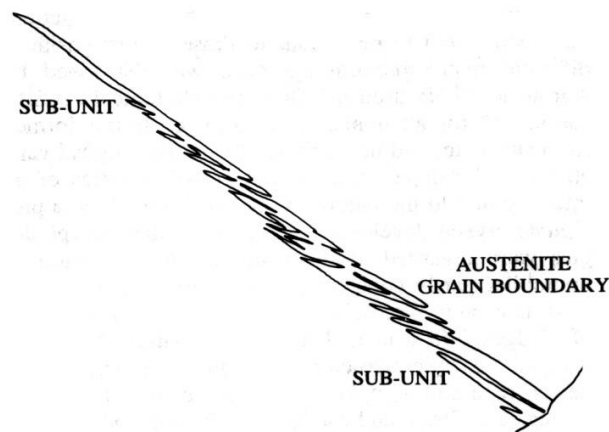


**Figure 1.7** Schematic illustration of the morphology of the sheaf [33].

The kinetics of bainite formation are influenced by several factors, including temperature, time, alloy composition, and cooling rate. By carefully controlling these

parameters during heat treatment, it is possible to tailor the microstructure and properties of the steel. As per the current understanding bainite are of three types: upper bainite, lower bainite and carbide-free bainite. Upper bainite and lower bainite are discussed in the section 1.2.1. The carbide-free nanostructured bainite is formed without any precipitation of carbide during low temperature austempering due to the addition of sufficient amount of silicon in the composition of material. Figure 1.8 depicts the influence of silicon on the fraction of cementite as a function of temperature. The mechanism of carbide-free bainite formation is discussed for Fe–1.2C–1.5Mn–1.5Si (mass%) steel and suggested that the equilibrium fractions of cementite are minimally affected by the presence of silicon. However, significant changes are observed under para-equilibrium conditions when silicon becomes trapped inside the cementite lattice and restricts its precipitation. It was reported that to prevent carbide precipitation at 250°C in a Fe-1.2C-Si-Mn alloy under para-equilibrium situations, a minimum of 2.0 mass% Si is necessary [34].

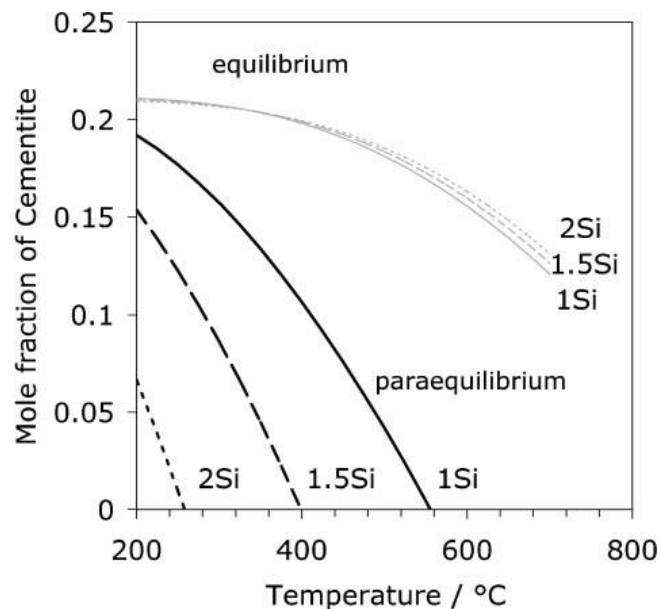


**Figure 1.8** Calculated phase fraction of cementite in equilibrium or para-equilibrium with austenite, in system Fe–Si–Mn–C with base composition Fe–1.2C–1.5Mn–1.5Si (mass%) [34].

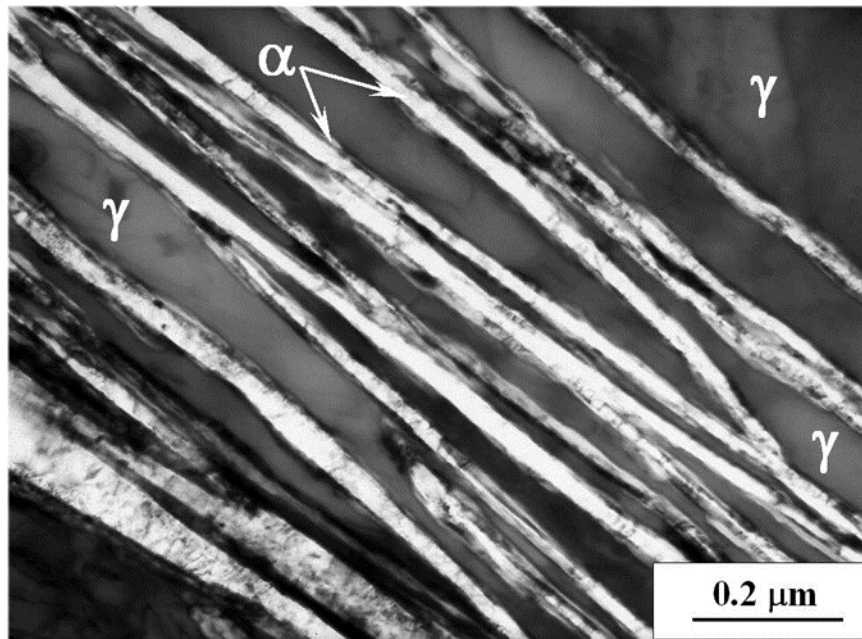


**Figure 1.9** Transmission electron micrograph of novel bainitic steel of composition Fe-0.98C-1.46Si-1.89Mn-0.26Mo-1.26Cr-0.09V austempered at 200°C for 5 days [35].

### 1.3 MICROSTRUCTURE AND TENSILE BEHAVIOUR

Nanostructured bainitic steels are developed for potential applications of wear-resistant components, rail and automobiles because of their promising properties of high wear resistance, strength, hardness, ductility and toughness [2, 36-40]. Medium carbon high silicon steel has higher martensite start temperature. To avoid martensite formation two-step austempering treatment is adopted which gives better fracture elongation [41]. Ausforming followed by austempering of high carbon steel accelerates bainitic ferrite transformation as well as produces higher stable retained austenite. In addition, the size of bainitic ferrite, both types of austenite and the content of blocky austenite are reduced and the bainitic ferrite is textured [42].

To meet most of the requirements scientists have designed a series of carbide-free bainitic steels with excellent mechanical properties in recent decades [16]. These are

typically high carbon (0.6-1) Fe alloys with small amount of Mn (0.7-2), Si>1.5, Cr (0.4-1.7), V (0-0.2), Mo (0-0.20), Al (0-1), Co (0-1.5) and Ni (0-2) (all are in mass %). Transformation of metastable austenite of the selected steel at the lowest possible temperature produces nanostructured bainitic ferrite which is carbide-free due to high silicon content with some amount of residual austenite to achieve high strength and high hardness [36, 43].

The residual austenite plays a complex role to achieve reasonable ductility and toughness. Quantity, size, shape or morphology, distribution, orientation, composition or chemical stability and mechanical stability of the residual austenite along with bainitic ferrite are critical for tailoring the ductility and toughness of the material. In general, optimum quantity, finer size, uniform distribution and higher chemical but lower mechanical stability provides higher ductility and toughness. The morphology of residual austenite between the subunits of the nanostructured bainitic plate is filmy but the retained austenite takes a blocky form between sheaves of bainitic ferrite. As the residual filmy austenite ( $\gamma_F$ ) is rich in carbon content [40, 44] due to its mechanism of formation, strain-induced martensitic (SIM) transformation is limited although in a few compositions the filmy austenite slowly transforms to martensite and results in reasonable ductility. The residual blocky austenite ( $\gamma_B$ ) contains lesser carbon and is chemically stable but mechanically more unstable on stressing.  $\gamma_B$  transforms to SIM under deformation. The material is strain hardened and plastic instability or onset of necking is delayed. The ductility of the material is improved due to transformation-induced plasticity (TRIP) [45]. Retained austenite volume fraction can be expressed in terms of applied strain( $e_p$ ), through a constant ( $k'$ ) by Equation (1).

$$\ln V_{RA}^{\circ} - \ln V_{RA} = k' e_p \quad (1)$$

where  $V_{RA}^{\circ}$  is the volume fraction of initial retained austenite,  $V_{RA}$  is the volume fraction of retained austenite after strain-induced martensitic transformation,  $k'$  is constant and is a function of the chemical composition of austenite and temperature of deformation or chemical free energy. More austenite stabilizing elements or temperature of deformation resist martensitic transformation.  $k'$  is proportional to the driving force for the transformation of austenite to SIM.

Lamellar austenite in multiphase medium carbon TRIP steel is beneficial to achieve the best combination of strength and ductility due to steady and gradual transformation to fine martensite but blocky austenite is detrimental due to abrupt transformation to coarse-sized martensite [46]. In high carbon nanostructured bainitic steel mechanical stability of retained austenite is more in compression than that in tension. Under compressive stress retained austenite transforms to martensite gradually compared to that of tension because of opposition by volume expansion associated with austenite to martensite transformation and that results in higher yield strength and higher ductility [47]. The low-temperature fracture toughness of high-carbon TRIP steel is higher and is aided by deformation-induced martensitic transformation during fracturing below  $M_d$  (the maximum martensite start temperature under deformation) [48].

Bainitic ferrite grows by a diffusionless mechanism. In a later stage, the excess carbon from bainitic ferrite is partitioned to nearby filmy austenite in between the plates. The enrichment of carbon makes the filmy austenite mechanically stable at a lower temperature. Retained austenite also presents in the form of blocky shapes and is lesser in carbon percentage than filmy austenite. Blocky austenite is mechanically unstable under applied stress and it transforms into brittle martensite, which made the steel brittle and therefore, it should be eliminated or reduced [36, 43, 49-52].

To reduce blocky austenite,  $T_0$  composition is shifted to higher composition and lower temperature [53]. The ductility can be improved by controlling the amount and type of filmy retained austenite [54-57]. Ductility can be further enhanced by transformation-induced plasticity (TRIP) by altering the mechanical stability of retained austenite.

Even though filmy austenite displays higher fracture toughness, as TRIP is limited because of high chemical and mechanical stability, the extent of work hardening or delaying in necking or ductility is also limited, unlike blocky austenite that responds strongly to TRIP.

There are plenty of studies/papers (Table 1) on steels with a high percentage (~90%) of nanostructure bainitic ferrite but properties like ductility and toughness are not up to the mark though high strength and high hardness are achieved in the ductile phase (retained austenite in the present case) content needs to be above the percolation limit of 10% [58]. The nanostructured bainitic steels can be classified into group 1 and group 2 as per bainitic ferrite content for discussion. Group 1 and group 2 bainitic steels consist of nanostructured bainitic ferrite of more than 86% and 66- 86%, respectively.

Nanostructured bainitic steel containing 87% bainitic ferrite (bainitic ferrite width less than 50 nm) was produced at an austempering temperature of 190°C. The microstructure contains the majority of 13% retained austenite as filmy morphology. The steels are reported to have compressive strength as high as 2500 MPa but it has low (compressive) ductility of <10% and a product of strength and elongation (PSE) value as low as 25 GPa% [36]. Nanostructured bainitic steels containing 87% or more bainitic ferrite are also produced in the austempering temperature range of 200-250°C. The microstructures contain retained austenite of less than 13 % of which the majority

(~12.9%) is in filmy form and a negligible amount of blocky austenite. In these steels, the carbon content in filmy austenite is high and the austenite is chemically as well as mechanically stable under straining. The microstructures reveal bainitic ferrite plate thickness in the range of 30-95 nm. The materials show tensile strength in the range of 1600-2375 MPa, total elongation in the range of 4.6 -11% and PSE values in the range of 10.02-19.8 GPa% [51, 54, 59]. In group 1 steels the major strength comes from the nanostructured bainitic ferrite and limited ductility is achieved because of low austenite content. The materials show low formability and energy-absorbing power due to low PSE values.

Steels with nanostructured bainitic ferrite of 66%-83.1% are synthesized in the austempering temperature range of 200-250°C. The microstructures show bainitic ferrite plate thickness in the range of 28-51 nm and the retained austenite in the range of 16.9 to 34% in which a comparable amount of filmy as well as blocky austenite is present. The material shows tensile strength in the range of 1400-2260 MPa, total elongation in the range of 6.8 -21.3% and PSE values in the range of 13.01-44.04 GPa% [35, 54, 59-61]. In general, group 2 steels have lower yield strength but tensile strength is very close to that of group 1. A significant part of strength comes from the martensite formed from the less mechanically stable blocky austenite due to strain-induced martensitic (SIM) transformation during deformation [54, 59, 60]. In addition, group 2 steels maintain higher ductility of which a significant part comes from the transformation-induced-plasticity (TRIP) of blocky austenite undergone SIM [54, 59, 60]. As a result, group 2 steels show higher formability and high energy absorbing power because of higher PSE values.

**Table 1.1** Microstructure parameters and mechanical properties of nanostructured bainitic steels

Steel Comp.	Aus. Tem p*, °C	V <sub>B</sub> %	t <sub>B</sub> , nm	V <sup>o</sup> <sub>RA</sub> , % (V <sup>F</sup> <sub>RA</sub> , %)	YS, MPa	UTS, MPa	TE, %	Hardness, HV	PSE GPa %	Ref
Group 1										
Fe-0.79C-1.59Si-1.94Mn-1.33Cr-0.30Mo-0.11V	190	87	<50	13	1959 (CPS)	2500 (CPS)	~10	650	25	[36]
Fe-0.8C-1.59Si-2.01Mn-0.24Mo-1Cr-1.51Co	200,	87	30	13, (12.9)	1410	2180	4.6		10.02	[54]
Fe-0.8C-1.84Si-2.18Mn-1.04Cr-0.3Mo-1.31Co-0.85Al	200	94.9	40-95	5.1		~1600-2000	~6-11	~610	~12-17.6	[51]
	250	90.4	30-80	9.6		~1500-1800	~1-13		~19.5-19.8	[51]
Fe-0.83C-1.56Si-1.37Mn-0.81Cr-1.44Al-0.87W	220	87.5	38	12.5	1955	2375	6.7		15.91	[59]
Group 2										
Fe-0.98C-1.46Si-1.89Mn-1.26Cr-0.26Mo-0.09V	200	69	35	31		2300		600		[35]
Fe-0.8C-1.59Si-2.01Mn-0.24Mo-1Cr-1.51Co	250,	79		21 (12)	1480	2060	19		39.14	[54]
Fe-0.79C-1.56Si-	200	83	45	17 (12.3)	1410	2260	7.6		17.17	[54]

1.98Mn- 0.24Mo- 1.01Cr- 1.51Co- 1.01Al	250	79		21 (12)	140 0	1930	9. 4		18.14	[54]
Fe-0.83C- 1.56Si- 1.37Mn- 0.81Cr- 1.44Al- 0.87W	240	83.1	51	16.9	182 6	2139	6. 8		14.54	[59]
Fe-0.98C- 2.9Si- 0.77Mn- 0.45Cr- 0.16Ni- 0.21Cu,	250	66	28	34	169 8	2068	21 .3	613	44.04	[60]
Fe-0.85C- 1.30Si- 1.92Mn- 0.29Mo- 2.05Co- 0.44Al	250	81.6	37	18.4	156 0	1807	7. 2	650	13.01	[61]

\*Aus. Temp.=austempering temperature, CPS=compressive strength

Findings on group 2 steels can be utilized to design group 3 steels (containing nanostructured bainitic ferrite of <66%) to get reasonably high strength and high hardness with significantly higher elongation and higher PSE values. It is worth studying nanostructured bainitic steel with a high amount of blocky austenite to improve ductility and toughness by TRIP and achieve significant strengthening by work hardening.

Therefore, the objectives of the present investigation are to produce nanostructured bainitic ferrite (55-65%) with a high amount of retained austenite to get a significant amount of ductility, strength and hardness and above all high product of strength and elongation (PSE). High PSE ensures significant strength, formability and enhanced energy-absorbing capabilities. In the present study tensile behaviour of nanostructured bainitic steel containing lower to a higher amount of blocky austenite is investigated. A new composition was designed to suppress the Ms temperature just above

room temperature and the addition of alloying elements Al and Co to increase the kinetics of bainitic transformation and its effect have been investigated on microstructure and mechanical properties.

#### 1.4 LOW CYCLE FATIGUE BEHAVIOUR

Numerous scientific studies have focused on the cyclic deformation of low and medium carbon bainitic steels in the plastic regime [62-67], whereas studies on the low cycle fatigue of high carbon nanostructured bainitic steels are extremely uncommon [68]. The results of the low cycle fatigue experiments conducted on high and medium carbon bainitic steels are presented in Table 3. The medium carbon steels have microstructural features that are slightly larger than 100 nm [63, 64, 67, 69], but they are discussed here due to the lack of low-cycle fatigue research on strictly nano-structured bainitic steels (feature-size less than 100 nm). In a study on the low cycle fatigue behaviour of a low carbon, carbide-free bainitic steel, Zhou et al. [67] found that the steels exhibited cyclic hardening followed by cyclic softening. Initial hardening was attributed to the high density of dislocations in the as-transformed microstructure and the decrease in mobile dislocation density due to their entanglement. Annihilation and rearrangement of dislocations were found to be the cause of cyclic relaxation during the final stages of fatigue life.

Zhao et al. [68] investigated the influence of varying the austempering time (0.5–4 h at 350 °C) within transformation status on the tensile and low cycle fatigue behaviours of a carbide-free nano-bainitic steel. With increasing austempering time, neither the microstructural length scale nor the size distribution of blocky-type RA changed. With a prolonged austempering duration, the most significant alterations observed were a decrease in the dislocation density of BF and carbon enrichment and homogenization in

RA. Under a different total strain amplitude value, both steels exhibited a similar stress response. At low total strain amplitude, initial cyclic hardening was followed by cyclic saturation and cyclic softening, whereas at higher total strain amplitude, initial cyclic hardening was followed by cyclic softening until failure. The steel austempered for an extended duration (4 h) exhibited a superior strength-ductility combination but a shorter fatigue life. It was due to (a) a reduced density of mobile dislocations in BF, resulting in a lower cyclic hardenability, and (b) blocky-type RA with a more homogeneous carbon distribution that transformed into a single martensite grain. Consequently, a localized incompatibility of elastic stresses developed at the interface between the newly formed martensite block and the BF lath. This resulted in initiation of fatigue cracks quickly and easily; thereby, reducing the fatigue life. Zhou et al. reported that at lower total strain amplitudes, the fatigue durations of the specimens increase with decreasing austempering temperature, whereas at higher total strain amplitudes, a comparable or even opposite result is observed [70]. During fatigue loading, blocky retained austenite with an inhomogeneous carbon distribution partially transforms into martensite, and the quantity of transformation increases with the total strain amplitude, particularly for specimens austempered at high temperatures. No study is available on the low cycle fatigue behaviour of high carbon carbide-free nanostructured bainitic steel.

### **1.5 IMPACT BEHAVIOUR**

In uniaxial tensile experiments of nanostructured bainitic steels, retained austenite transforms into the harder strain-induced martensite that results in transformation induced plasticity (TRIP effect) and increasing the work hardening capacity of the material [39, 71]. Consequently, the strength-ductility ratio is determined by the morphology and volume fraction of the phases present in the microstructure.

However, the impact resistance of nanostructured bainitic steels will determine whether or not they can be used in engineering applications. Therefore, it is necessary to investigate the effect of morphology and volume fraction of phases on the impact toughness of nano-bainitic steels. B. Avishan et al. [72] reported the impact energy trend in relation to austempering temperature and demonstrated that the toughness maximum occurs at intermediate temperatures. The lower toughness at higher austempering temperatures was attributed to the coarse morphology of retained austenite, whereas the degraded toughness at the lowest temperature was attributed to an inadequate volume fraction of ductile austenite phase. B. Garbarz et al. discovered that specimens subjected to martensitic transformation exhibited a greater impact durability than specimens created using standard treatment [73]. This enhancement in resilience was attributed to a refinement of the bainite/retained austenite structure, which was driven by a decrease in the prior austenite grain size. M. J. Peet et al. [74] have enhanced the toughness–strength combinations by decreasing the grain size of prior austenite. Kumar et al. studied the effect of austempering temperature on Charpy impact energy of the nanostructured bainitic steel and reported that the impact energy increases from 7 J to 15 J when austempering temperature increases from 250 to 350°C [61]. However, very limited study is available on the impact energy of nanostructured bainitic steel with higher fraction of retained austenite.

## 1.6 TRIBOLOGICAL BEHAVIOUR

As a result of the expansion of rail transportation in recent years, the deployable speed of trains has continually grown. Moreover, axle load, passenger movement, and cargo volume have all consistently increased, which has led to an increase in the expenditures associated with rail and wheel maintenance and replacement [1, 75]. In

order to accommodate these rigorous operating conditions, the materials used for wheels and rails need to have their tensile strength, resistance to wear, and fatigue resistance increased proportionately. Previously, pearlitic steels were utilized as rail material. In spite of this, a number of publications have suggested that bainitic steels may be comparable to pearlitic steels in terms of the wear resistance they exhibit when subjected to rolling contact fatigue and adhesion [76, 77]. It is general fact that a certain type of bainitic steel must possess both a high level of strength and a good toughness in order to achieve an exceptional level of wear resistance. This is especially true for steels that have been alloyed with silicon [78, 79]. Because of their high levels of strength, ductility, and toughness, high carbon, high silicon steels with bainitic structures are useful for a variety of applications in the locomotive and automotive sectors [80-84]. In addition to their superior mechanical properties, high carbon, silicon bainitic steels are promising for wear applications [33, 85-88]. The use of bainitic steel was also recommended for the high wear conditions in railroad applications [33]. It was reported that the wear resistance of high C and Si bainitic steel with coarse globular carbides reveals better tribological performance than the 100Cr6 steel with tempered martensite structure [85]. Due to the improved hardness, they found that a further decrease in austempering temperature might be advantageous for wear resistance. Guo et al. have also reported that 0.83% C-2.44% Si bainitic steel has a higher resistance to wear than tempered martensitic steel [86]. Abrasive wear of austempered medium carbon steel induces martensite in the retained austenite which hardens the matrix and improves wear resistance [80]. It was demonstrated that bainitic steels withstand abrasion better than martensitic steels of comparable hardness and chemical composition [89]. From the combination of ductility and hardness, Hurricks discovered that lower bainite had high abrasion resistance [90]. Experiments on two-body abrasion were carried out by Xu and Kennon on plain carbon

steels that had a wide range of compositions (0.10 to 1.4 wt.% C) and microstructures. They noted that bainite had the highest wear resistance for C concentrations of less than 1.0 wt.%, followed by tempered martensite and the remaining annealed structures. The wear resistance of spheroidized structures is found to be the lowest [91]. Abrasion tests carried out on South African soil revealed that lower bainite had greater abrasion resistance than other microstructures [92]. It is assumed that the superior abrasion resistance observed in bainitic steel is attributable to less plastic deformation wear as a result of its high toughness during three-body abrasion [93]. Though, there are contradicting findings that the wear resistance of bainitic steel under two-body abrasion has been shown to be one third of pearlitic steel, possibly as a result of the lower bainite having a weak strain-hardening rate [94, 95]. Kritika et al. reported that specific wear rate of the high carbon (0.89 wt.%C) carbide-free nanostructured bainitic steels decreases with reduction in thickness of the bainite plate. The coefficient of frictions decreases with increase in cycles and the blocky retained austenite transformed to filmy retained austenite during the frictional sliding and also decrease in hardness at the subsurface [96]. Chen et al. showed that under conditions of sliding wear, residual austenite was no longer stable and underwent transition into strain-induced martensite [37]. According to reports by Neetu et al. [97], in multi-phase steel, bainite that was created by austempering without continuous cooling techniques demonstrated the maximum wear resistance; this was the case regardless of the austempering temperatures. Tribological behaviour of high carbon carbide-free nanostructured bainitic steels is not yet understood fully. Further studies are required to resolve conflicting findings in tribological performance of bainitic steels.

## 1.7 CORROSION BEHAVIOUR

In contemporary rail applications, the development of hard and tough, high strength, abrasion- and corrosion-resistant bainitic steels is seen as the leading research trend [98, 99]. Heat treatment methods can be utilized to alter the microstructure of steel to enhance its mechanical and corrosion properties [83, 101-104]. The pearlitic eutectoid steel is normally utilized in rail applications [102]. The normal rail steel has a lamellar structure of pearlite, and its strength could be enhanced by heat-treatment techniques and appropriate alloying [103, 104]. The presence of a substantial quantity of cementite in the microstructure of pearlite makes the structure more susceptible to corrosion [99, 105, 106]. Recent development has produced a rail steel, micro-alloyed with Cr, Cu and Ni with a pearlitic microstructure, which reveals enhanced resistance to atmospheric and crevice corrosion [99]. Consequently, several researchers have studied rail steel with new phases containing nanostructured bainite and retained austenite (RA) [83, 107]. Bainite-based rail steel possesses superior mechanical properties compared to those with a pearlitic one [83]. Nanostructured bainitic steels (NSB steels) have demonstrated ultra-high yield and tensile strength, considerable fracture toughness, and wear resistance [61, 107-110]. Precipitation of carbides in bainite at low temperature austempering can be inhibited by the addition of a sufficient amount of silicon [34].

The steel that is used for rail applications is susceptible to several forms of corrosion in a variety of conditions, including localized, general, and microbiological forms of corrosion. Since these issues have become more common [111-113], efforts have been made to manufacture better corrosion-resistant steels. The corrosion resistance of steel is mostly influenced by the alloy composition and microstructure. Si, C, Mn, Ni, Cu, and Cr alloying elements significantly modify corrosion behaviour by influencing microstructure, stability of passive layer, the form of the corrosion product and its

composition [114-120]. The investigators have examined the comparative corrosion performance of rail steels with varied morphologies of pearlite and bainite resulting from different heat treatment procedures [83, 103, 111, 121]. According to Hiasch et al., the different phases of the steel may significantly affect the electrochemical dissolution behaviour [100]. The distinct dissolution behaviour of cementite and ferrite phases is a result of their unique electrode potentials, which result in the creation of galvanic couples [122]. Moreover, it was reported that at higher carbon levels, bainitic steel has greater corrosion resistance than pearlitic one. Additionally, it has been found that, compared to the bainitic phase, the ferrite phase possesses a greater activity and dissolution rate [123]. The enrichment of alloying elements like Cr and Cu at the interface between the corroded surface and the substrate is attributed to the improvement in the corrosion resistance of the low-carbon bainitic steel [120]. The enrichment of these elements causes adherence and compactness of the corrosion layer to the metal substrate. It has been found that NSB steel has a stronger polarization resistance than martensitic one [124]. It has been reported that low-carbon steel displays superior corrosion resistance than high-carbon one during electrochemical impedance spectroscopy and salt fog exposure studies for almost two months [106]. Improved corrosion resistance in low C steel was attributed to the homogeneous distribution of bainite and ferrite in the microstructure, which resulted in the development of a uniform, compact passive layer early in the corrosion period. Austempered medium carbon high silicon alloy containing 10.7 vol% retained austenite provides good corrosion resistance [125]. The corrosion resistance of nanostructured materials is adversely affected by electrolytes that promote the production of stable passive films [126]. The development of micro galvanic couple is hindered, and the characteristics of the oxide layer are increased owing to the fine and uniform distribution of phases, and it has a significant effect on the corrosion resistance of the material [121,

127, 128]. Kazum et al. have studied the effect of austempering temperature on electrochemical corrosion behaviour of NSB steels in aqueous 3.5% NaCl. They reported that corrosion current density has decreased with a lowering in Austempering Temperature and a large content of coarser retained austenite led to selective dissolution during galvanostatic polarization test [129]. During electrochemical impedance spectroscopy (EIS) and potentiodynamic polarization test in a 3.5 wt.% NaCl solution, it was observed that an enhancement in the corrosion current density as well as shifting of potential towards the active side with respect to the increase in Austempering Temperature, reduction in  $R_{ct}$  and loss in pure capacitance [130]. It was reported that at a certain isothermal temperature, the corrosion rate of a newly developed multiphase steel increases initially with increasing continuous cooling time, then decreases as pearlite begins to form [131]. Singh et al. have found that corrosion resistance of NSB steels in an aqueous 3.5% NaCl for 30 days improved with reduction in the Austempering Temperature [132].

In rail clips, lower bainite structure with 30% retained austenite and small fraction of cementite is reported to have higher corrosion resistance than that of tempered martensite structure due to high carbon carbide networks in the tempered material. With increase in austempering time fraction of bainite increases and amount of retained austenite decreases [133]. The corrosion resistance of medium carbon bainitic steels was enhanced by boro-austempering treatment [134]. Austempered multi-phase bainitic/martensitic steels provide better corrosion resistance than the commercial pearlitic steel [135]. Increasing austempering temperature resulted in lesser bainite fraction and higher content of blocky martensite/austenite (M/A) island and the corresponding bainitic steel display lower corrosion resistance due to the decreasing average carbon content of retained

austenite and enhanced residual stress induced by the formation of blocky M/A island [136]. Though limited literatures are available on corrosion behaviour of 0.86 % carbon carbide free nanostructured bainitic steel with low retained austenite content [132], however, there is no significant study available in literature on corrosion behaviour of high carbon carbide-free nanostructured bainitic steel with high amount of retained austenite as well as with variation of austempering time.

### **1.8 KNOWLEDGE GAPS**

Very few studies are available on the effect of higher amount of retained austenite on tensile properties of high carbon carbide-free nanostructured bainitic steels. No study is available on the LCF behaviour of high carbon carbide-free nanostructured bainitic steel. There is hardly any literature on tribological behaviour of high carbon carbide-free nanostructured bainitic steels. There is no significant study available in literature on corrosion behaviour of high carbon carbide-free nanostructured bainitic steel with high amount of retained austenite.

### **1.9 OBJECTIVES OF THE PRESENT INVESTIGATION**

The objectives of the present investigation are:

- Design and characterization of ultrahigh strength carbide-free nanostructured bainitic steel at lowest possible austempering temperature.
- Ductilization, strengthening and toughening of high carbon nanostructured bainitic steel.
- Evaluation of low cycle fatigue behaviour of high carbon nanostructured bainitic steel.
- To study the dry sliding wear behaviour of nanostructured bainitic steel.

- To study the effect of microstructure on Electrochemical and immersion Corrosion behaviour of nanostructured bainitic steel.